Configuration of Guard Band and Offsets in Cyclic Queuing and Forwarding

Damien Guidolin–Pina, Marc Boyer, Jean-Yves Le Boudec

Configuration of Guard Band and Offsets in Cyclic Queuing and Forwarding

Damien Guidolin--Pina, Marc Boyer, and Jean-Yves Le Boudec

Abstract—Cyclic Queuing and Forwarding (CQF) is a mechanism defined by IEEE TSN for providing low jitter in a deterministic network. CQF uses a common time cycle and two buffers per node output port: during one cycle incoming packets are stored in one buffer while packets in the other buffer are being transmitted; at the end of a cycle, the roles of the two buffers are exchanged. The cycle start times are determined by a time offset that may be different for every output buffer. A guard band at both cycle ends is devised in order to compensate for misalignment and timing inaccuracies. The proper operation of CQF requires that the guard band and the offsets are computed such that nodes are sufficiently time-aligned. First, we give necessary and sufficient conditions for this to be guaranteed. The sufficient conditions lend themselves to tractable computations and we show that they are close to optimal. Our conditions account for nonideal clocks and non-zero propagation times; we show that accounting for these two elements does matter. Second, we give a method for computing the minimal duration of the guard band, given prior choices of time offsets. Third, a judicious choice of time offsets can considerably decrease the required duration of the guard band: we give a practical algorithm, based on a Mixed Integer Linear Program, for computing offsets that minimize the guard band. We illustrate our results on several CQF network topologies with or without cyclic dependencies.

Index Terms—TSN; CQF; Peristaltic Shaper; Cyclic Queuing and Forwarding.

1 Introduction

In order to offer a standard real-time data network, the IEEE Time Sensitive Networking working group has defined several extensions to Ethernet. Among others, Cyclic Queuing and Forwarding (CQF), previously known as "peristaltic shaper", has been defined in order to offer guaranteed delay and limited jitter [1]. In short (see Section 2 for more details), CQF considers a common time cycle, T, and uses two queues per node output port to alternatively store or forward frames. It guarantees that the delay experienced by a frame crossing h switches along its path is between $(h-1)T$ and $(h+1)T$.

CQF has appealing characteristics: it is simple to implement, it offers a simple expression of the latency bound, it provides a limited delay jitter ($2T$) [2] and can also easily handle cyclic dependencies (whereas other real-time mechanisms may require some attention is such cases, [3]–[5])

Nevertheless, it requires some time synchronization and alignment of cycles between switches [2]. Moreover a fraction of the cycle time is used by a "guard band", S, (called "adjustment factor" in [1]), that absorbs the effects of imperfections in time synchronization and alignment, and during which the output port can not be used by CQF frames. To avoid this issue, several alternative strategies have been defined (cf. Section 7), but they all require at least a third queue, or even a fourth one. Furthermore, the cycle start times are determined by a time offset that may be different for every output buffer.

The use of CQF requires the choice of two network-wide parameters, the cycle time T and the guard band S, and of the values of all time offsets at output buffers. The cycle time is related to the flows characteristics, whereas the guard band and the time offsets are related to synchronization between switches. In this paper, we address the choice of time offsets and guard band.

We consider the clock error model from [6], which captures the effects of clock nonidealities in the context of deterministic networks (cf. Section 3). Then we provide:

- a formal characterization of CQF cycle alignment and guard band (Sections 3 and 4.1), where, unlike other studies, we do not assume that all cycle offsets are equal;
- two sufficient conditions to check if a guard band S is large enough (Section 4.1), one being a simplification of the other;
- a necessary condition (Section 4.2), which is used to show the quality of the sufficient conditions (Section 4.3);
- a method to compute the minimum value of the guard band, given some pre-specified values of time offsets (Theorem 2);
- three strategies to compute a common guard band and local time offsets (two analytic ones, and a third using a Mixed Integer Linear Program – MILP – in Section 5);
- an evaluation of the strategies on some synthetic benchmarks, in Section 6.

The experiments of Section 6 show that:

- clock nonideality cannot be neglected;
- the choice of the offsets may have a dramatic effect on the minimum guard band value.

- *Damien Guidolin--Pina is with RealTime-at-Work.*
- *Marc Boyer is with ONERA/DTIS, Université de Toulouse – F-31055 Toulouse – France.*
- *Jean-Yves Le Boudec is with EPFL.*

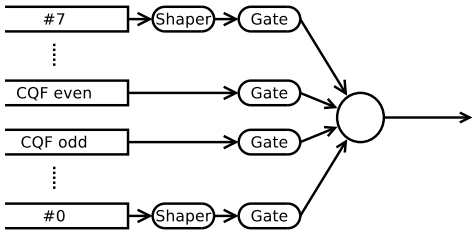

Fig. 1: Queues of a bridge using CQF policy.

2 Presentation of CQF

2.1 Alternating Cycles

Consider a node offering a CQF policy to a set of flows (a CQF class) on a given output port. Two queues, called "even" and "odd" are dedicated to this CQF class, as depicted in Figure 1. The CQF node has a periodic behaviour, with period T (called "cycle time"), which has the same value for all CQF nodes in the network. Let $c(t)$ denote the value displayed at the clock of the node when the true time is t and let o be the time offset at this server. A time instant t is said to be in an "even" [resp. "odd"] cycle if $\left\lfloor \frac{c(t)-o}{T} \right\rfloor$ is even [resp. odd][1]. During an even cycle, the even queue is served and all received frames are stored in the odd queue. The frames stored in the odd queue will be forwarded in the next odd interval. The same holds, mutatis mutandi, with odd cycles.

The operation of CQF on an illustrative topology is shown in Figure 2. Under correct operation, CQF provides two guarantees: if a frame follows a path made of h hops, the end-to-end delay is in the range $[(h-1)T, (h+1)T]$ and the delay-jitter is upper bounded by $2T$ (for example, any frame of stream s1 experiments a delay in T and $3T$). For correct operation, two conditions must be satisfied [7]. First, at every node, it must be possible to transmit in one cycle all frames received in the previous cycle. This requires that there is enough link capacity to support the rates of all sources and that the cycle duration is large enough to absorb the burstiness of all incoming flows in one cycle. This condition and the resulting minimum cycle length is studied in companion work and is outside the scope of this paper. Second, the cycles of consecutive nodes must be aligned such that all frames sent by a node when a buffer is open for transmission can be stored by the receiving node in a buffer that is open for reception. This condition is discussed in the next subsection.

2.2 Time-Aligned Nodes and Guard Band

In a CQF network, nodes are assumed to be time-synchronized. However, propagation times and switchover time (from switch input to switch output) are non zero and time synchronization is never perfect. To compensate for these effects, the standard introduced a guard band S at the beginning and at the end of each cycle as illustrated in Figure 3. The value of S is the same for all CQF nodes in the network.

The figure shows two frames, F and F', sent by N_i to N_j with their emission time (E and E') and their propagation

1. An expression such as $\lfloor x \rfloor$ denotes the floor of x.

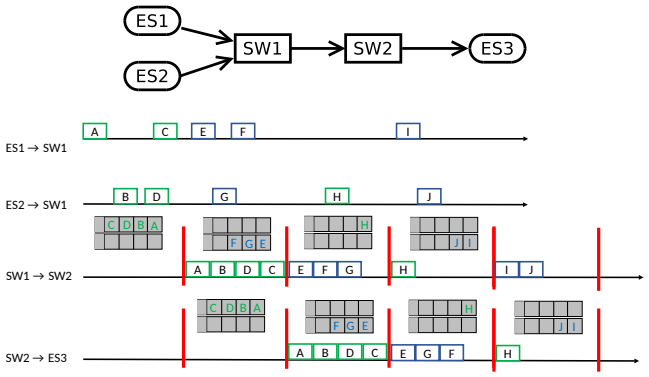

Fig. 2: Operation of CQF on an illustrative topology.

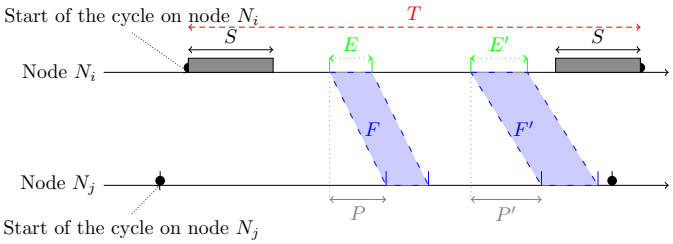

Fig. 3: Illustration of the guard time S.

times (P and P'). Here both cycles are not aligned. This can be by design (e.g. to compensate for propagation time) but can also occur due to clock imperfections.

The standard states that "S should be set to the sum of the errors or jitter values from all sources given in [a] list" and gives a list of sources of errors [1, §T.5.3]. In Section 4, we formally define what "Time-Aligned Nodes" means and give practical conditions to ensure that the time alignment holds. The conditions bear on the values of the guard band and the offsets. The guard band may result in a waste of capacity, hence it should be minimized. In Section 5 we give methods to compute offsets and guard band that minimize the guard band.

2.3 Other Aspects of CQF

The implementation of CQF relies on two mechanisms, the Per-Stream Filtering and Policing at input port (PSFP, [8]) and the Gate Control List at output port (GCL) defined in the "Enhancements for Scheduled Traffic" extension of the IEEE 802.1Q bridging standard [9]. PSPF has a time-driven table (also called GCL) which forwards the CQF frames from the input to the even or odd buffer on the output port. During an open interval, a queue has to compete with the other queues, using the static priority policy.

Then, the cycle time must account for higher priority flows and some limited interaction with lower priority flows to ensure that the frames received in the previous cycle can be forwarded in the current cycle. The conditions on the cycle time are out of the scope of this paper.

During the guard band, some higher or lower priority frames can be transmitted. Higher priority frames can be transmitted at any time, in or outside the guard band. Lower priority frame can start either during the guard band, or outside the guard band, once the current CQF queue

is empty. When no preemption is implemented [10], the blocking factor is $\frac{l_{lp}^{\max}}{C}$ where $l_{lp}^{\max}$ is the maximal size of a lower priority packet and C the link bandwidth. If the preemption is implemented, and if the CQF queue is marked as "express" and the lower priority flow is "preemptable", the blocking factor can be reduced to $\frac{143*8}{C}$ [11].

The standard also considers the case with several CQF classes having different cycle time and illustrates an example of interleaving in [1, Fig. T-5], presented also in [12]. Moreover, in wide area networks, some papers have proposed to extend CQF to more than 2 buffers. Such extensions are out of the scope of this paper.

3 System Model and Notation

We consider a network with a single CQF class with two buffers and n nodes $N_1 ... N_n$. The CQF cycle time is T; there is a guard band of duration S at the beginning of every cycle, and one of same duration at the end. The nominal values of T and S are identical at all nodes. In contrast, the links may have different bit rates $R_{i,j}$. Table 1 gathers the notation used throughout the paper.

Obviously, there must be enough time in one cycle to transmit the largest possible frame, i.e. we assume that

$$T - 2S \geq \max_{i,j} \overline{E}_{i,j}. \tag{1}$$

where $\overline{E}_{i,j}$ is the transmission time of a frame of maximum size on the link from N_i to N_j. The same way, $\underline{E}_{i,j}$ is the transmission time of a frame of minimum size on the link from N_i to N_j.

Every node has a local clock and all clocks are synchronized, using for example the protocol specified in [13]. However, at the microsecond time scale, synchronization is not perfect and clock non idealities have to be taken into account. We use the following model, taken from [6]. Let $c_i(t)$ be the local time displayed by the clock of node N_i when the true time (international atomic time, TAI) is t. The nonideality of clock c_i can be characterized by the clock stability bound $\rho_i \geq 1$, the timing jitter bound $\eta_i \geq 0$ and the synchronization error bound Δ_i, such that displayed times satisfy:

$$\forall t, d \geq 0 : \frac{d - \eta_i}{\rho_i} \leq c_i(t+d) - c_i(t) \leq d\rho_i + \eta_i, \tag{2}$$

$$\forall t \geq 0 : |c_i(t) - t| \leq \Delta_i. \tag{3}$$

The former equation captures the effect of clock drift, jitter and wander on measurements of time intervals performed with the local clock. The latter equation captures the effect of the time synchronization protocol. In a TSN network synchronized with gPTP (generic PTP), the maximal admissible values are $\rho_i = 1.0001$ [13, Annex B.1.1], $\eta_i = 2$ns [13, Annex B.1.3.1] and $\Delta_i = 1\mu$s [13, Section B.3]. The characteristics of network components can be found in component data-sheets, freely available (e.g. [14], [15]) or reserved to customers. The two equations above can be combined, which leads to the following bound on the measurements of time intervals (proof in Appendix B):

$$\max \begin{cases} d - 2\Delta_i \\ \frac{d-\eta_i}{\rho_i} \end{cases} \leq c_i(t+d) - c_i(t) \leq \min \begin{cases} d + 2\Delta_i \\ d\rho_i + \eta_i \end{cases} \tag{4}$$

TABLE 1: Notation

$\overline{E}_{i,j} = \frac{\overline{L}_{i,j}}{R_{i,j}}$	Max transmission time of CQF frame from N_i to N_j
$\underline{E}_{i,j} = \frac{\underline{L}_{i,j}}{R_{i,j}}$	Min transmission time of CQF frame from N_i to N_j
$k \in \mathbb{N}$	Index of a cycle
$\underline{L}_{i,j}, \overline{L}_{i,j}$	Min, max size of CQF frames from N_i to N_j
$L_{i,j}^{\text{NPr}}$	Maximum size of high priority frame from N_i to N_j
N_i	Node i
o_i	Time offset at node i
$\underline{P}_{i,j}, \overline{P}_{i,j}$	Lower and upper bounds on propagation time
P	Mean propagation time $P = \frac{1}{2}\left(\overline{P}_{i,j} + \underline{P}_{i,j}\right)$
p	Propagation jitter parameter, $p = \frac{1}{2}\left(\overline{P}_{i,j} - \underline{P}_{i,j}\right)$
$R_{i,j}$	Bit rate of link from N_i to N_j
S	Duration of guard band at begin and end of cycle
T	Duration of cycle
$\underline{z}_j, \overline{z}_j$	Lower and upper bounds on switching time
$c_i(t)$	time displayed by clock of N_i when true time is t
Δ_i	clock synchronization error bound (e.g. $\Delta_i = 1\mu$s)
$\rho_i \geq 1$	clock stability bound (e.g. $\rho_i = 1.0001$)
$\eta_i \leq 2\Delta$	clock timing jitter bound (e.g. $\eta_i = 2$ns)
$\lfloor x \rfloor$	floor of the real number x
$m\%2$	residual modulo 2 of the integer m
ε	a tolerance on the accuracy of floating-points
$\overline{S}$	a network-wide upper bound on S, (15)
$\underline{S}$	a lower bound on $\mathcal{S}_{\text{thm1}}^{o_i,o_j}$, (16)
$S_{\text{thm1}}^{*o_i,o_j}, S_{\text{thm1}}^{*}$	minimum value of S (at precision ε) that satisfies the sufficient condition in Theorem 1
$S_{\text{cor1}}^{*o_i,o_j}, S_{\text{cor1}}^{*}$	minimum value of S (at precision ε) that satisfies the simpler sufficient condition in Corollary 1
$\underline{S}_{\text{cor1}}^{o_i,o_j}$	infimum of all values of S that satisfy Corollary 1; may or may not be feasible and $0 \leq S_{\text{cor1}}^{*o_i,o_j} - \underline{S}_{\text{cor1}}^{o_i,o_j} \leq \varepsilon$
$S_{\text{thm3}}^{*o_i,o_j}, S_{\text{thm3}}^{*}$	minimum value of S (at precision ε) that satisfies the necessary condition in Theorem 3
I	number of nodes
$\mathcal{L}$	set of links

Also note that we can always assume that $2\Delta \geq \eta$ since otherwise we can replace η by 2Δ (Property 1 in Appendix C).

Node N_i uses a time offset o_i, at which the initial cycle begins. Consequently, the kth cycle starts at this node at true time t_k^i such that $c_j(t_k^i) - o_j = kT$. Thus, at true time t, node N_i is in the kth cycle with $k = \left\lfloor \frac{c_j(t) - o_j}{T} \right\rfloor$.

For a CQF frame F that travels from N_i to N_j, let t_{em}^F denote the instant at which node N_i finishes transmitting the last bit of F. Unless otherwise specified, all time instants are in true time. Then, node N_j receives the frame F and a classifier chooses in which queue the frame will be forwarded. Let t_{cl}^F denote the instant at which the frame F is forwarded to the queue $Q_{j,b}$ of the node N_j with $b = \left\lfloor \frac{c_j(t_{cl}^F) - o_j}{T} \right\rfloor \%2$ (where $\%2$ denotes the remainder modulo 2). Note that the choice is done when the frame is totally received in the node N_j. The difference $P_{i,j}^F = t_{cl}^F - t_{em}^F$ is the sum of the propagation time from N_i to N_j plus the time for ingress processing and is simply called "propagation" in the rest of the paper. Then, the frame is transmitted through the

switch fabric and is written in the queue $Q_{j,b}$. Let t^F_{wr} denote the instant when the last bit of the frame F is written in the queue $Q_{j,b}$ of node N_j. Note that the frame is written during the cycle $\left\lfloor \frac{c_j(t^F_{wr})-o_j}{T} \right\rfloor$. The difference $z^F_j = t^F_{wr} - t^F_{cl}$ is called the switching time. Figure 4 illustrates these definitions.

Following [1], we assume that the propagation time is not constant but has some bounded variability; this may correspond to variable decoding and processing times. Let $\underline{P}_{i,j}, \overline{P}_{i,j}$ be lower and upper bounds on the propagation time from N_i to N_j. The difference $\overline{P}_{i,j} - \underline{P}_{i,j}$ is a bound on the "propagation jitter". Similarly, we assume that the switching time has some bounded variability and let $\underline{z}_j, \overline{z}_j$ denote lower and upper bounds on the switching time at N_j.

In [16, § 4.11.3], it is specified that the "technological latency of the switch should be less than 100 μs." At the time of writing, a value of 15μs seems acceptable.

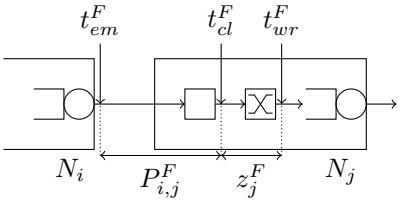

Fig. 4: Significant times between 2 nodes N_i and N_j.

4 Conditions for Time Alignment

In this section we solve the issue of time alignment of nodes. This involves the offsets and the guard band. The main results of this section are Theorem 1 and Corollary 1, which give sufficient conditions for nodes to be time aligned; the latter is more tractable than the former and gives the basis of methods to compute offsets and minimal guard band that minimize the duration of the guard band in Section 5. We also show in Theorem 2 that the minimum value of the guard band for given offsets can be obtained by binary search. Ideally, we would like to have a necessary and sufficient condition, but this appears to be out of reach as it is difficult to quantify all possible behaviours; instead, we give a necessary condition and show that the difference with the sufficient condition is small. In the idealized case where clocks are perfect and switching latency is negligible, the conditions are identical.

4.1 Sufficient Conditions

We start by a formal definition of time alignment.

Definition 1 (Time aligned nodes)**.** *Consider a node N_i that has a link to a node N_j. We say that N_i and N_j are time-aligned if and only if, for any cycle index k at N_i, there exists a cycle index k' at N_j such that all frames sent by N_i in cycle k are forwarded by node N_j in cycle k' out of a single CQF buffer.*

Using the notation in Section 3, we have that a frame sent at time t to the node j is classified at time t_{cl} in the queue $Q_{j,b}$ with $b = \left\lfloor \frac{c_j(t_{cl})-o_j}{T} \right\rfloor \%2$ and received at time t_{wr} in this queue during the cycle $k = \left\lfloor \frac{c_j(t_{wr})-o_j}{T} \right\rfloor$.

Consequently, Definition 1 is equivalent to saying that, for any two frames F, F' sent by N_i to N_j during one same cycle, they are classified in the same queue $Q_{j,b}$, with

$$b = \left\lfloor \frac{c_j(t^F_{cl}) - o_j}{T} \right\rfloor \%2 = \left\lfloor \frac{c_j(t^{F'}_{cl}) - o_j}{T} \right\rfloor \%2 \tag{5}$$

and they are received in the same cycle k with

$$k = \left\lfloor \frac{c_j(t^F_{wr}) - o_j}{T} \right\rfloor = \left\lfloor \frac{c_j(t^{F'}_{wr}) - o_j}{T} \right\rfloor \tag{6}$$

Using Equations (5) and (6), we obtain the following sufficient condition:

Theorem 1 (Sufficient condition for node alignment)**.** *Consider two nodes N_i, N_j such that N_i has a link to N_j. The parameters $\eta_i, \eta_j, \rho_i, \rho_j, \Delta_i, \Delta_j, \underline{E}_{i,j}, o_i, o_j, S$ and T are as defined in section 3. Define $U_{i,j}(S)$ and $L_{i,j}(S)$ by*

$$L_{i,j}(S) = S + \underline{E}_{i,j} + \underline{P}_{i,j} + o_i - o_j - (\Delta_i + \Delta_j) - \widehat{l}_{i,j}(S) \tag{7}$$

with

$$\widehat{l}_{i,j}(S) = \min \begin{cases} (\underline{E}_{i,j} + S) \cdot (1 - \frac{1}{\rho_i}) + \frac{\eta_i}{\rho_i} + 2\Delta_j, \\ 2\Delta_i + 2\Delta_j, \\ (\underline{E}_{i,j} + S) \cdot (1 - \frac{1}{\rho_i \cdot \rho_j}) \\ \qquad + \underline{P}_{i,j} \cdot (1 - \frac{1}{\rho_j}) + \frac{\eta_i}{\rho_i \cdot \rho_j} + \frac{\eta_j}{\rho_j}, \\ (\underline{E}_{i,j} + S + \underline{P}_{i,j}) \cdot (1 - \frac{1}{\rho_j}) + \frac{\eta_j}{\rho_j} + 2\Delta_i \cdot \frac{1}{\rho_j} \end{cases} \tag{8}$$

and

$$U_{i,j}(S) = T - S + \overline{P}_{i,j} + \overline{z}_j + o_i - o_j + \Delta_i + \Delta_j + \widehat{u}_{i,j}(S) \tag{9}$$

with

$$\widehat{u}_{i,j}(S) = \min \begin{cases} (T - S) \cdot (\rho_i - 1) + \eta_i + 2\Delta_j \\ 2\Delta_i + 2\Delta_j \\ (T - S) \cdot (\rho_i \cdot \rho_j - 1) + \eta_i \cdot \rho_j \\ \qquad + (\overline{P}_{i,j} + \overline{z}_j) \cdot (\rho_j - 1) + \eta_j \\ (T - S + \overline{P}_{i,j} + \overline{z}_j) \cdot (\rho_j - 1) + \eta_j + 2\Delta_i . \rho_j \end{cases} \tag{10}$$

If the parameters satisfy the condition

$$\left\lfloor \frac{U_{i,j}(S)}{T} \right\rfloor = \left\lfloor \frac{L_{i,j}(S)}{T} \right\rfloor \tag{11}$$

then, the two nodes N_i, N_j are time aligned and the difference between the emission and the reception cycles is constant, equal to

$$\delta^{i,j} = \left\lfloor \frac{U_{i,j}(S)}{T} \right\rfloor = \left\lfloor \frac{L_{i,j}(S)}{T} \right\rfloor \tag{12}$$

If all clocks are perfect, the values of L and U become

$$L_{i,j}(S) = S + \underline{E}_{i,j} + \underline{P}_{i,j} + o_i - o_j, \tag{13}$$

$$U_{i,j}(S) = T - S + \overline{P}_{i,j} + \overline{z}_j + o_i - o_j. \tag{14}$$

The condition (11) then expresses that the guard band S and the offsets o_i, o_j have to compensate the transmission, propagation and switching delays. With nonideal clocks, there are additional terms in L and U: the former term, $\Delta_i + \Delta_j$, captures the synchronization accuracy whereas the

latter term, namely $\widehat{l}$ or $\widehat{u}$, captures the effect of supplementary nonidealities. The values in the theorem then add some margin in order to account for clock nonidealities.

The term $\delta^{i,j}$ represents the difference in cycle number. At first glance, one may expect, up to some normalisation, to always have $\delta^{i,j} = 0$, *i.e.* a frame sent a cycle k is received at cycle k. But as will be shown in the experiments (Section 6, Figure 20), one may introduce some phase between the offsets to absorb the propagation time and reduce the guard band. When this strategy is used on a non feed-forward network (a network with cycles) with large propagation time (*i.e.* when the sum of the propagation times is more than half of the cycle time T), some non null $\delta^{i,j}$ will appear.

Sketch of proof. The proof consists in bounding the reception time of frames sent by the node N_i to the node N_j in one cycle. To this end, we consider two frames, the former being sent as early as possible and the latter as late as possible. Let t, t' be the respective reception instants. Since both have to be received in the same cycle, it is implied that $\left\lfloor \frac{c_j(t)-o_j}{T} \right\rfloor = \left\lfloor \frac{c_j(t')-o_j}{T} \right\rfloor$ (where c_j is the clock of N_j). Then, we use the conditions on clocks to compute a lower bound on the former expression and an upper bound on the latter.

The full proof is given in Appendix D. □

The values of $L_{i,j}(S)$ and $U_{i,j}(S)$ depend on S in a non-linear way. In Section 5 we are interested in computing offsets that minimize S; this non-linearity leads to MILPs with many binary variables, which quickly become intractable. This motivates us to derive from Theorem 1 the simpler sufficient condition in Corollary 1, which, as we show in Section 4.3, remains very close. To this end, first observe that, by (1), we must have

$$S \leq \overline{S} := \frac{T - \max_{i,j} \overline{E}_{i,j}}{2} \tag{15}$$

Second, we use the following lower bound:

Property 1. *Let*

$$\underline{\underline{S}} := \max_{i,j} \left(\frac{\overline{P}_{i,j} + \overline{z}_j - \underline{P}_{i,j} - \underline{E}}{2} + \Delta_i + \Delta_j \right) \tag{16}$$

If S satisfies the sufficient condition (11) *in Theorem 1 for every pair i, j, then $S > \underline{\underline{S}}$.*

Proof. The proof is given in Appendix E. □

This leads to the following, simpler, sufficient condition:

Corollary 1 (Simpler Sufficient Condition for Node Alignment)**.** *Theorem 1 continues to hold if we replace $\widehat{l}_{i,j}(S)$ and $\widehat{u}_{i,j}(S)$ by $\widehat{l}_{i,j}(\overline{S})$ and $\widehat{u}_{i,j}(\underline{\underline{S}})$, i.e. if we replace $L_{i,j}(S), U_{i,j}(S)$ by*

$$L'_{i,j}(S) = S + \underline{E}_{i,j} + \underline{P}_{i,j} + o_i - o_j - (\Delta_i + \Delta_j) - \widehat{l}_{i,j}(\overline{S}) \tag{17}$$

$$U'_{i,j}(S) = T - S + \overline{P}_{i,j} + \overline{z}_j + o_i - o_j + \Delta_i + \Delta_j + \widehat{u}_{i,j}(\underline{\underline{S}}) \tag{18}$$

Proof. The proof is given in Appendix F. □

Next, we study the set of values of the guard time S that, for given values of the offsets o_i, o_j, satisfy the sufficient condition in Theorem 1 or in Corollary 1. Specifically, we are interested in minimizing the value of S for given values of the offsets, which is given by the next theorem.

Theorem 2. *For given values of the offsets o_i, o_j, let $\mathcal{S}_{\text{thm1}}^{o_i,o_j}$ be the set of values of $S \in [0; \overline{S}]$ that satisfy the sufficient condition* (11) *in Theorem 1.*

- *$\mathcal{S}_{\text{thm1}}^{o_i,o_j}$ is not empty if and only if $\overline{S}$ satisfies* (11)*;*
- *If $\mathcal{S}_{\text{thm1}}^{o_i,o_j}$ is not empty then there exists some $\underline{S}_{\text{thm1}}^{o_i,o_j} > 0$ such that*

$$\mathcal{S}_{\text{thm1}}^{o_i,o_j} = \left(\underline{S}_{\text{thm1}}^{o_i,o_j}; \overline{S}\right]$$

$$\text{or } \mathcal{S}_{\text{thm1}}^{o_i,o_j} = \left[\underline{S}_{\text{thm1}}^{o_i,o_j}; \overline{S}\right].$$

- *If $\mathcal{S}_{\text{thm1}}^{o_i,o_j}$ is not empty, let $S_{\text{thm1}}^{*o_i,o_j}$ be the smallest value of $S \in \mathcal{S}_{\text{thm1}}^{o_i,o_j}$ obtained with binary search in the interval $[0; \overline{S}]$ with precision ε (this requires $\left\lceil \log_2 \frac{\overline{S}}{\varepsilon} \right\rceil$ steps). Then $S_{\text{thm1}}^{*o_i,o_j}$ is an ε-over-approximation of $\underline{S}_{\text{thm1}}^{o_i,o_j}$. i.e. $[S_{\text{thm1}}^{*o_i,o_j}; \overline{S}] \subset \mathcal{S}_{\text{thm1}}^{o_i,o_j}$ and $S_{\text{thm1}}^{*o_i,o_j} - \underline{S}_{\text{thm1}}^{o_i,o_j} \leq \varepsilon$.*

The same holds mutatis mutandi with Corollary 1.

The proof is in Appendix G. The above theorem establishes that the set of feasible guard band durations is an interval; however, it may be closed or semi-closed, i.e. it is not certain that the infimum is feasible. This is because of the floor in (11), which leads to a discontinuous condition (see Lemma 8 in Appendix K for details). This means that, strictly speaking, there might not be a minimum value. In practice, however, we are interested in values expressed with some accuracy, say ε, and the theorem means that, modulo a precision of ε, there is a minimum value $S_{\text{thm1}}^{*o_i,o_j}$, and any value above it and below $\overline{S}$ is feasible. The same holds for the condition in Corollary 1, and since any S that satisfies Corollary 1 also satisfies Theorem 1, we always have $S_{\text{thm1}}^{*o_i,o_j} \leq S_{\text{cor1}}^{*o_i,o_j}$. Furthermore, we show numerically in Section 4.3 that the difference is small.

Last, the following property (proof in Appendix H) shows that the sufficient condition models the expected notion of slack: improving a clock can only reduce the value of the required guard band.

Property 2. *Let S be a solution of Theorem 1 with two clock quality parameters $(\rho_i, \eta_i, \Delta_i)$ $(\rho_j, \eta_j, \Delta_j)$ for some values of the offsets o_i, o_j. Then, S is also a solution with better clock quality parameters $(\rho'_i, \eta'_i, \Delta'_i)$ $(\rho'_j, \eta'_j, \Delta'_j)$ for the same values of the offsets o_i, o_j. Here better means $\rho'_i \leq \rho_i$, $\eta'_i \leq \eta_i$, $\Delta'_i \leq \Delta'_i$, $\rho'_j \leq \rho_j$, $\eta'_j \leq \eta_j$, $\Delta'_j \leq \Delta'_j$. The same holds mutatis mutandi with Corollary 1.*

4.2 Necessary Condition

We now complement the sufficient condition in the previous section with a necessary condition. For readability, in this subsection we drop the dependency on i, j in U and L variables.

Theorem 3 (Necessary condition for time alignment)**.** *Let N_i, N_j be two nodes with parameters $\eta_i, \eta_j, \rho_i, \rho_j, \Delta_i, \Delta_j, \underline{E}_{i,j}, o_i, o_j, S$ as defined in Section 3. Define $X, s, \tilde{L}_{\%}, \tilde{L}_{\%s}, \tilde{U}_{\%}, \tilde{U}_{\%s}, \tilde{L}, \tilde{L}_s, \tilde{U}$ and $\tilde{U}_s$ as follow:*

$$X = \underline{P}_{i,j} - \Delta_i + o_i - o_j + \underline{E} + S \tag{19}$$

$$\tilde{L}_{\%} = X - \Delta_j \tag{20}$$

$$\tilde{L} = X - \Delta_j + \min \begin{cases} \underline{z}_j + 2\Delta_j, \\ \rho_j \cdot \underline{z}_j + \eta_j \end{cases} \tag{21}$$

$$\tilde{U}_{\%} = X + \min \begin{cases} T - \underline{E} - 2S + \overline{P}_{i,j} - \underline{P}_{i,j} + \Delta_j + 2\Delta_i \\ (T - \underline{E} - 2S) \cdot \rho_i + \overline{P}_{i,j} - \underline{P}_{i,j} + \Delta_j \\ (T - \underline{E} - 2S + \overline{P}_{i,j} - \underline{P}_{i,j} + 2\Delta_i) \cdot \rho_j + \eta_j - \Delta_j \\ ((T - \underline{E} - 2S) \cdot \rho_i + \overline{P}_{i,j} - \underline{P}_{i,j}) \cdot \rho_j + \eta_j - \Delta_j \end{cases} \tag{22}$$

$$\tilde{U} = X + \min \begin{cases} T - \underline{E} - 2S + \overline{P}_{i,j} - \underline{P}_{i,j} + \overline{z}_j + \Delta_j + 2\Delta_i \\ (T - \underline{E} - 2S) \cdot \rho_i + \overline{P}_{i,j} - \underline{P}_{i,j} + \overline{z}_j + \Delta_j \\ (T - \underline{E} - 2S + \overline{P}_{i,j} - \underline{P}_{i,j} + \overline{z}_j + 2\Delta_i) \cdot \rho_j \\ \qquad + \eta_j - \Delta_j \\ ((T - \underline{E} - 2S) \cdot \rho_i + \overline{P}_{i,j} - \underline{P}_{i,j} + \overline{z}_j) \cdot \rho_j + \eta_j - \Delta_j \end{cases} \tag{23}$$

$$s \in \{-1\ ;\ 1\} \tag{24}$$

$$\tilde{L}_{\%s} = E + S + \underline{P} + o_i - o_j - s \cdot (\Delta_i + \Delta_j) \tag{25}$$

$$\tilde{L}_s = \tilde{L}_{\%1} + \underline{z} \tag{26}$$

$$\tilde{U}_{\%s} = T - S + \overline{P} + o_i - o_j - s \cdot (\Delta_i + \Delta_j) \tag{27}$$

$$\tilde{U}_s = \tilde{U}_{\%1} + \overline{z} \tag{28}$$

If the two nodes N_i, N_j are time aligned for any valid clock trajectory and $\eta \leq \underline{E}_{i,j}$, then :

$$\left\lfloor \frac{\tilde{U}}{T} \right\rfloor = \left\lfloor \frac{\tilde{L}}{T} \right\rfloor \text{ and } \left\lfloor \frac{\tilde{U}_{\%}}{T} \right\rfloor \%2 = \left\lfloor \frac{\tilde{L}_{\%}}{T} \right\rfloor \%2 \tag{29}$$

$$\text{and } \left\lfloor \frac{\tilde{U}_s}{T} \right\rfloor = \left\lfloor \frac{\tilde{L}_s}{T} \right\rfloor \text{ and } \left\lfloor \frac{\tilde{U}_{\%s}}{T} \right\rfloor \%2 = \left\lfloor \frac{\tilde{L}_{\%s}}{T} \right\rfloor \%2 \tag{30}$$

and the difference between the emission and the reception cycle is constant, equal to $\delta^{i,j}$ with

$$\delta^{i,j} = \left\lfloor \frac{\tilde{U}}{T} \right\rfloor = \left\lfloor \frac{\tilde{L}}{T} \right\rfloor \tag{31}$$

An illustration of Theorem 3 is provided in Figure 5. When clocks are perfect, the values become

$$\tilde{L}_{\%} = \tilde{L}_{\%s} = S + \underline{E}_{i,j} + \underline{P}_{i,j} + o_i - o_j = L \tag{32}$$

$$\tilde{U}_{\%} = \tilde{U}_{\%s} = T - S + \overline{P}_{i,j} + o_i - o_j = U - \overline{z}_j \tag{33}$$

$$\tilde{L} = \tilde{L}_s = S + \underline{E}_{i,j} + \underline{P}_{i,j} + \underline{z}_j + o_i - o_j = L + \underline{z}_j \tag{34}$$

$$\tilde{U} = \tilde{U}_s = T - S + \overline{P}_{i,j} + \overline{z}_j + o_i - o_j = U. \tag{35}$$

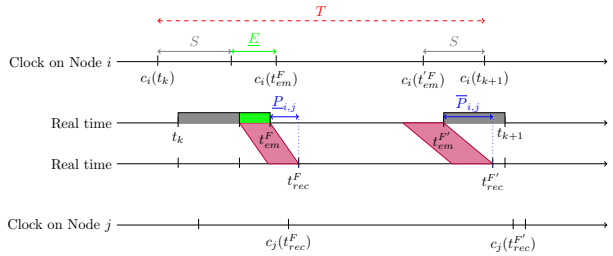

Fig. 5: Illustration of Theorem 3.

TABLE 2: Random Parameters (μs) for Figure 6. Nodes i, j are fixed, $o_i = 0$, $\underline{P}_{i,j} = P - p$ and $\overline{P}_{i,j} = P + p$.

Random values (in μs, except for ρ, unitless)			
P	p	$\overline{z}_j$	$\underline{z}_j$
$[0; 200]$	$[0.01; 0.1] * P$	$[0; 15]$	$[0; \overline{z}]$
o_j	Δ	ρ	η
$[0; 1000]$	$[0; 1]$	$1 + [0; .0002]$	$[0; .002]$

Sketch of proof: . The proof uses adversarial frame emission patterns as well as clock behaviours. It consists in sending a first frame F in the first cycle of N_i as soon as possible, just after the opening guard band, and a second frame F' as late as possible, just before the closing guard band. In the proof, t_0 denotes the instant when the first cycle starts (*i.e.* $c_i(t_0) - o_i = 0$), and t_1 is the instant when the last bit of F is sent (*i.e.* $c_i(t_1) = c_i(t_0) + S + \underline{E}$), and t_2 the instant when the last bit of F' is sent (*i.e.* $c_i(t_2) = c_i(t_0) + T - S$). Let t^F_{rec}, $t^{F'}_{rec}$ denote the reception instants of F and F'. In order to maximize the difference between $c_j(t^F_{rec})$ and $c_j(t^{F'}_{rec})$, while satisfying the set of constraints, we consider that the clock c_i runs as fast as possible on $[t_0; t_1]$ and as slowly as possible on $[t_1; t_0 + T]$ while the clock c_j runs as fast as possible from t^F_{rec}, as illustrated in Figure 5.

The full proof is given in Appendix I. □

For given values of the offsets o_i, o_j, let $\mathcal{S}^{o_i,o_j}$ be the set of values of S that satisfy the exact but intractable conditions in (5), (6) and let $\mathcal{S}^{o_i,o_j}_{\text{thm3}}$ be the set of values of S that satisfy the necessary condition of Theorem 3. It follows that

$$\mathcal{S}^{o_i,o_j}_{\text{thm3}} \subset \mathcal{S}^{o_i,o_j} \subset \mathcal{S}^{o_i,o_j}_{\text{thm1}} \subset \mathcal{S}^{o_i,o_j}_{\text{cor1}} \tag{36}$$

In the next section we will compare these sets. Note that, while $\mathcal{S}^{o_i,o_j}_{\text{thm1}}$ and $\mathcal{S}^{o_i,o_j}_{\text{cor1}}$ are intervals, it is not clear whether the same holds for $\mathcal{S}^{o_i,o_j}_{\text{thm3}}$ and $\mathcal{S}^{o_i,o_j}$. However, let $\underline{S}^{o_i,o_j}_{\text{thm3}} = \inf \mathcal{S}^{o_i,o_j}_{\text{thm3}}$, which we numerically compute by brute force, thus obtaining an ε-lower approximation $S^{*o_i,o_j}_{\text{thm3}}$. It follows that the length of $\mathcal{S}^{o_i,o_j} \setminus \mathcal{S}^{o_i,o_j}_{\text{thm1}}$ is upper bounded by $S^{*o_i,o_j}_{\text{thm1}} - S^{*o_i,o_j}_{\text{thm3}}$, which thus bounds the pessimism of the sufficient condition in Theorem 1 (and similarly with Corollary 1).

4.3 Comparing the Three Conditions

We have obtained two sufficient conditions (Theorem 1 and Corollary 1) and one necessary condition (Theorem 3). To evaluate the tightness of the sufficient conditions, we compute the values of $S^{*o_i,o_j}_{\text{thm1}} - S^{*o_i,o_j}_{\text{thm3}}$ and $S^{*o_i,o_j}_{\text{cor1}} - S^{*o_i,o_j}_{\text{thm1}}$ for different values of the offsets and other parameters taken randomly with a uniform distribution in the intervals shown in Table 2.

We take 100000 configurations using these parameters and we compute $S^{*o_i,o_j}_{\text{thm1}}$ and $S^{*o_i,o_j}_{\text{cor1}}$ by binary search (with $\varepsilon = \overline{S} \cdot 10^{-10}$) and $S^{*o_i,o_j}_{\text{thm3}}$ by scanning all values between 0 and S^*_{thm1} with a step of 10 ns for each configuration. Note that for 3978 configurations there is no solution, i.e. the parameters don't allow to find any valid guard band value. We trace the histogram shown on Figure 6 of the difference between the values (see x label).

As we can see, the two sufficient conditions are close: The maximum difference between them is around 0.2 μs and

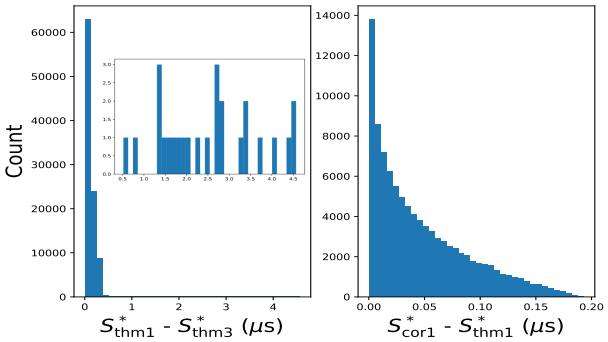

Fig. 6: Histogram of the difference between the conditions.

the average difference is around 0.05 μs. Thus, the condition in Corollary 1 is satisfactory because it is easier to compute and quite close to Theorem 1.

Moreover, we see that the difference between the sufficient and the necessary condition is around 0.1 μs and the maximum difference is around 4.5 μs. However, on this set of configurations, only 26 values are greater than 0.5 μs (0.03 % of the configurations, visible on the zoom of the left graph). Thus, we can consider that we are close enough to the true (intractable) solution by using the sufficient condition.

4.4 Effect of Clock Nonidealities

The incorporation of clock nonidealities brings some complexity to the analysis. In this section we test whether such a modelling accuracy is really necessary. We consider a representative configuration as in Table 3 and consider the effect of the following three factors in the analysis: (1) propagation jitter $2p$ and switching time $\overline{z}$; (2) clock synchronization error Δ; (3) clock jitter and drift parameters ρ, η. This leads to the following four scenarios:

- 'Perfect': propagation jitter and switching times are null and clocks are perfect. This is the assumption done in most of the literature.
- 'Perfect clock, default other': propagation jitter and switching times are considered but clocks are perfect.
- 'Default': considers all elements described in this paper.
- 'Default, synchronization only': result of a simplified analysis that captures clock synchronization accuracy but ignores bounds on clock jitter and drift.

The resulting S^* are computed as in the previous section, and the results are shown in Table 3. We observe that, with the perfect configuration, all the resulting S^* are approximately equal to 0 (not exactly, due to the tolerance ε). However, with the other scenarios, the resulting S^* are all non negligible and cause a loss of about 3-4 percent of the cycle time for this single configuration. Most of it comes from system delays (3%), and clock errors add another .5%. Last, ignoring clock drift and jitter bounds induces an increase in the guard band by .5% for the sufficient conditions and increases the gap between the necessary and the sufficient condition. Thus, the model including the clock drift and jitter bounds is significantly better than the one only considering the clock synchronization.

TABLE 3: Effect of clock nonidealities. Nodes i, j are fixed, $\underline{P}_{i,j} = P - p$ and $\overline{P}_{i,j} = P + p$.

Values for all scenarios.				
T	P	$\underline{z}_j$	o_i	o_j
1ms	100μs	0	0	100μs
$\underline{E}_{ij}$		$\overline{E}_{ij}$		
0.672μs		12.384μs		

	Perfect	Perfect clock, default other	Default	Default, synchronization only
p	0	0.5 μs	0.5 μs	0.5 μs
$\overline{z}_j$	0	15 μs	15 μs	15 μs
Δ	0	0	1 μs	1 μs
ρ	1	1	1.0001	$+\infty$
η	0	0	2 ns	$+\infty$
S^*_{cor1}	2.9e-8 μs	15.5 μs	17.7 μs	21.5 μs
S^*_{thm1}	2.9e-8 μs	15.5 μs	17.7 μs	21.5 μs
S^*_{thm3}	2.9e-8 μs	15.5 μs	17.5 μs	17.5 μs

This suggests that we can't ignore the nonidealities; this is confirmed by the thorough experiments in Section 6.

5 Computing the Guard Band and the Offsets

In the previous section we have shown that Corollary 1 obtains a quasi-optimal condition to decide whether some guard band value S is admissible and gives a method to test whether some feasible guard band exists at all. Furthermore, we have shown that there is an infimal value $\underline{S}^{o_i,o_j}_{\text{cor1}}$, for given values of time offsets o_i, o_j, which may or may not be admissible, but such that any value in the range $(\underline{S}^{o_i,o_j}_{\text{cor1}}; \overline{S}]$ is admissible with respect to the constraints on link (i, j). We have also given a method to compute an ε over-approximation, $S^{*o_i,o_j}_{\text{cor1}}$, of $\underline{S}^{o_i,o_j}_{\text{cor1}}$, which can be interpreted as a minimal guard band value, given offsets.

If the values of the offsets are imposed or given by some oracle, the infimal guard band is then equal to $\max_{(i,j)\in\mathcal{L}} \underline{S}^{o_i,o_j}_{\text{cor1}}$, since it must satisfy the constraints on every link. However, as we show below, the values of the time offsets largely influence the infimal guard band. Therefore, we are interested in solving

$$\begin{aligned} &\textbf{Problem } (P)\text{:} \\ &\text{minimize} \max_{(i,j)\in\mathcal{L}} \underline{S}^{o_i,o_j}_{\text{cor1}} \\ &\text{over} (o_i)_{i=1:I} \in [0; T]^I \end{aligned}$$

where, by convention, $\underline{S}^{o_i,o_j}_{\text{cor1}} = +\infty$ if Corollary 1 gives no admissible guard band for these values of o_i, o_j. In the above, $\mathcal{L}$ is the set of links and I is the number of nodes. If Problem (P) has a solution, say $\underline{S}$, then any S that satisfies $\underline{S} < S \leq \overline{S}$ is a valid guard band.

We first give two simple heuristics that correspond to common practices; then we derive a MILP formulation of Problem (P).

5.1 Heuristics

Recall that the condition in Corollary 1 is:

$$\left\lfloor \frac{U'_{i,j}(S)}{T} \right\rfloor = \left\lfloor \frac{L'_{i,j}(S)}{T} \right\rfloor \tag{37}$$

where $L'_{i,j}, U'_{i,j}$ are defined in (17) and (18).

5.1.1 Null offset

This solution consists in aligning all offsets, which, without loss of generality, can be written as $o_i = o_j = 0$. The condition in (37) becomes:

$$\begin{aligned} &\left\lfloor \frac{S + \underline{E}_{i,j} + \underline{P}_{i,j} - (\Delta_i + \Delta_j) - \widehat{l}_{i,j}(\overline{S})}{T} \right\rfloor \\ &= \left\lfloor \frac{T - S + \overline{P}_{i,j} + \overline{z}_{i,j} + \Delta_i + \Delta_j + \widehat{u}_{i,j}(\underline{\underline{S}})}{T} \right\rfloor \end{aligned} \tag{38}$$

The general case is complicated (see Appendix J), but can be considerably simplified when the cycle time is large compared to propagation and transmission. Specifically, consider the following condition, stating that the clock error term $\hat{l}_{i,j}$ is small with regards to emission, propagation and switching times, which also are smaller than the cycle time:

$$0 \leq \underline{E}_{i,j} + \underline{P}_{i,j} + \overline{P}_{i,j} + \overline{z}_{i,j} + \widehat{u}_{i,j}(\underline{\underline{S}}) - \widehat{l}_{i,j}(\overline{S}) < T. \tag{39}$$

If this condition holds for every i, j, then the floor functions in (38) are null (see Appendix J, (242)), implying

$$0 \leq S + \underline{E}_{i,j} + \underline{P}_{i,j} - (\Delta_i + \Delta_j) - \widehat{l}_{i,j}(\overline{S}) < T \tag{40}$$
$$0 \leq T - S + \overline{P}_{i,j} + \overline{z}_{i,j} + \Delta_i + \Delta_j + \widehat{u}_{i,j}(\underline{\underline{S}}) < T. \tag{41}$$

Consequently,

$$S \geq (\Delta_i + \Delta_j) + \widehat{l}_{i,j}(\overline{S}) - \underline{E}_{i,j} - \underline{P}_{i,j} \tag{42}$$
$$S > \overline{P}_{i,j} + \overline{z}_{i,j} + \Delta_i + \Delta_j + \widehat{u}_{i,j}(\underline{\underline{S}}) \tag{43}$$

However, since (39) holds, then

$$\overline{P}_{i,j} + \overline{z}_{i,j} + \widehat{u}_{i,j}(\underline{\underline{S}}) \geq \widehat{l}_{i,j}(\overline{S}) - \underline{E}_{i,j} - \underline{P}_{i,j} \tag{44}$$

It follows that the infimum of S is

$$S_{\text{null}} = \max_{i,j} \left\{ \overline{P}_{i,j} + \overline{z}_{i,j} + \Delta_i + \Delta_j + \widehat{u}_{i,j}(\underline{\underline{S}}) \right\}, \tag{45}$$

i.e. if (39) holds for every i, j and $S_{\text{null}} < \overline{S}$, then any S in $(S_{\text{null}}; \overline{S}]$ is an admissible value for the guard band.

As expected, the guard band needs to absorb terms related to the clock imperfections (Δ_i, Δ_j, $\widehat{u}_{i,j}(\underline{\underline{S}})$) but it also has to absorb the maximal propagation and maximal switching times ($\overline{P}_{i,j}$, $\overline{z}_{i,j}$).

In the general case (when (39) does not hold for some i, j) the expression of S_{null} is more complicated and is given in Appendix J.

5.1.2 Absorbing the propagation with offsets

The standard suggests to set the guard band such that it compensates the "jitter in the propagation time", whereas the expression in eq. (45) involves the propagation itself, not its jitter. This suggests another strategy, where the offsets are set to compensate the average propagation time.

Let P be the mid propagation time between the node i and the node j, and $p_{i,j}$ the semi-variation, i.e.:

$$P_{i,j} = \frac{\underline{P}_{i,j} + \overline{P}_{i,j}}{2}, \quad p_{i,j} = P_{i,j} - \underline{P}_{i,j} = \overline{P}_{i,j} - P_{i,j}. \tag{46}$$

Assume that we can choose o_i and o_j such that

$$o_j = o_i + P_{i,j} \tag{47}$$

then the condition 37 becomes:

$$\begin{aligned} &\left\lfloor \frac{S + \underline{E}_{i,j} - p_{i,j} - (\Delta_i + \Delta_j) - \widehat{l}_{i,j}(\overline{S})}{T} \right\rfloor \\ &= \left\lfloor \frac{T - S + p_{i,j} + \overline{z}_{i,j} + \Delta_i + \Delta_j + \widehat{u}_{i,j}(\underline{\underline{S}})}{T} \right\rfloor \end{aligned} \tag{48}$$

As Equation (1) is respected, we know that

$$\begin{aligned} S + \underline{E}_{i,j} - p_{i,j} - (\Delta_i + \Delta_j) - \widehat{l}_{i,j}(\overline{S}) &\quad (49)\\ \leq \underline{E}_{i,j} + S &\quad (50)\\ \leq T - S < T \text{ because } S > 0. &\quad (51) \end{aligned}$$

So, it comes $\left\lfloor \frac{S + \underline{E}_{i,j} - p_{i,j} - (\Delta_i + \Delta_j) - \widehat{l}_{i,j}(\overline{S})}{T} \right\rfloor = 0$. Consequently, $\left\lfloor \frac{T - S + p_{i,j} + \overline{z}_{i,j} + \Delta_i + \Delta_j + \widehat{u}_{i,j}(\underline{\underline{S}})}{T} \right\rfloor = 0$, thus

$$T - S + p_{i,j} + \overline{z}_{i,j} + \Delta_i + \Delta_j + \widehat{u}_{i,j}(\underline{\underline{S}}) < T \tag{52}$$
$$S > p_{i,j} + \overline{z}_{i,j} + \Delta_i + \Delta_j + \widehat{u}_{i,j}(\underline{\underline{S}}). \tag{53}$$

It follows that the infimum of S is

$$S_{\text{prop}} = \max_{i,j} \left\{ \frac{\overline{P}_{i,j} - \underline{P}_{i,j}}{2} + \overline{z}_{i,j} + \Delta_i + \Delta_j + \widehat{u}_{i,j}(\underline{\underline{S}}) \right\}. \tag{54}$$

In other words, if for every link (i, j) : $o_j = o_i + \frac{\overline{P}_{i,j} + \underline{P}_{i,j}}{2}$, and $S_{\text{prop}} < \overline{S}$, then any S in $(S_{\text{prop}}; \overline{S}]$ is an admissible value for the guard band.

As expected, the guard band needs to absorb terms related to the clock imperfections (Δ_i, Δ_j, $\widehat{u}(\underline{\underline{S}})$) but it also has to absorb the jitter of the propagation time and the maximal switching time.

However, having (47) simultaneously at all links i, j is not always possible, for example when a switch has several inputs or in case of cyclic dependency (in case of a ring).

5.1.3 Comparing the Two Heuristics

Observe that $S_{\text{prop}} < S_{\text{null}}$, i.e. setting the offsets to absorb the propagation time, when it is possible, always gives a smaller (i.e. better) guard band than when aligning all offsets. For a single pair of nodes, the difference is $\frac{\overline{P}_{i,j} + \underline{P}_{i,j}}{2}$, i.e. the median propagation delay. Considering a propagation speed being 60% of light speed, as in [17, N.6] (that is to say, 0.18m/ns) it takes 0.11μs to cross a 20m cable, and in a Metropolitan Area Network (MAN), a 20km cable will have a transmission delay of 0.11ms. At 1Gb/s, 0.11ms is the transmission time of 110Kb of data.

The fact that S_{prop} can be significantly smaller than S_{null} indicates that the time offsets do have an important effect on the minimum guard band. However, the heuristic that leads to S_{prop} imposes strict constraints on the network topology, and is often not applicable. This motivates us to find a solution to Problem (P), i.e. to compute time offsets that minimize the guard band.

5.2 Using a MILP Solver

In this section we derive a method to solve Problem (P). First notice that, from (37), Problem (P) is equivalent to

Problem (P'):
minimize
over $S \in [0; \overline{S}],\ (o_i)_{i=1:I} \in [0;T]^I$,
subject to $\left\lfloor \frac{U'_{i,j}(S)}{T} \right\rfloor = \left\lfloor \frac{L'_{i,j}(S)}{T} \right\rfloor, \forall (i,j) \in \mathcal{L}$

(Note that, in the above, $L'_{i,j}, U'_{i,j}$ depend on o_i, o_j.)

Because we always have $L'_{i,j} \leq U'_{i,j}$, the last condition is equivalent to

$$\left\lfloor \frac{L'_{i,j}(S)}{T} \right\rfloor \geq \left\lfloor \frac{U'_{i,j}(S)}{T} \right\rfloor, \tag{55}$$

which, by Property 3 in Appendix E, is equivalent to

$$\exists k_{i,j} \in \mathbb{Z}, k_{i,j} \leq \frac{L'_{i,j}(S)}{T} \text{ and } \frac{U'_{i,j}(S)}{T} < k_{i,j} + 1. \tag{56}$$

Therefore, Problem (P') is equivalent to

Problem (P''):
minimize S (57)
over $S \in [0; \overline{S}],\ (o_i)_{i=1:I} \in [0;T]^I, (k_{i,j})_{(i,j)\in\mathcal{L}} \in \mathbb{Z}^{\mathcal{L}}$
subject to
$k_{i,j} \leq \frac{L'_{i,j}(S)}{T},\ \frac{U'_{i,j}(S)}{T} < k_{i,j} + 1, \forall (i,j) \in \mathcal{L}$

Because of the strict inequality in its last condition, Problem (P'') is ill-posed (its infimum might not be attained) and cannot be solved as is by MILP solvers. To circumvent this, we replace it by the following MILP, in which the strict inequality is modified to an inclusive inequality, using the same tolerance ε as before:

Problem $(P{-}\text{MILP})$:
minimize S
over $S \in [0; \overline{S}],\ (o_i)_{i=1:I} \in [0;T]^I, (k_{i,j})_{(i,j)\in\mathcal{L}} \in \mathbb{Z}^{\mathcal{L}}$
subject to
$k_{i,j} \leq \frac{L'_{i,j}(S)}{T},\ \frac{U'_{i,j}(S)}{T} \leq k_{i,j} + 1 - \frac{\varepsilon}{T}, \forall (i,j) \in \mathcal{L}$

The following theorem establishes that Problem $(P{-}\text{MILP})$ provides an ε-over-approximation of the infimum of Problem (P), as required.

Theorem 4. *Let S_{MILP} be the optimum value of S returned by Problem $(P{-}\text{MILP})$. It is an ε-over-approximation of the value $\underline{S}$ returned by Problem (P), i.e. $0 \leq S_{\text{MILP}} - \underline{S} \leq \varepsilon$. Furthermore, the values of S_{MILP} and of the offsets returned by S_{MILP} are valid.*

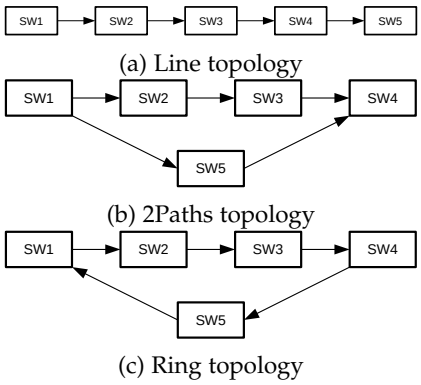

Fig. 7: Three simple graphs

TABLE 4: Parameters used with the three topologies in Figure 7.

Constant values		
T	$\underline{E}$	ϵ
0.001s	$6.72 * 10^{-7}$s	10^{-10}

Perfect values					
P	p	$\overline{z}$	Δ	ρ	η
0.05ms	0	0	0	1	0

Default values					
P	p	$\overline{z}$	Δ	ρ	η
0.05ms	0.5μs	15μs	1μs	1.0001	2 ns

The proof is in Appendix K.

It follows that we can use a MILP solver with Problem $(P{-}\text{MILP})$ and obtain the minimal value of the guard band S at precision ε, together with the values of the offsets. Specifically, if Problem $(P{-}\text{MILP})$ is feasible, the returned valued of S_{MILP} and of the offsets are valid and S_{MILP} is optimal at precision ε. Note that for Problem (P) it is not certain that the optimal value $\underline{S}$ is valid because we don't know in general whether the infimum of Problem (P) is attained; the last statement in the theorem recalls that such a complication may not happen with Problem $(P{-}\text{MILP})$.

6 Experiments

In this section we apply the two heuristics and the MILP formulation to the three network topologies in Figure 7 and compare the corresponding optimal values of guard bands, namely, S_{null}, S_{prop} and S_{milp}. The goal of the simple topologies is to illustrate the feasibility of our tools, to obtain some feelings for the values of the guard band, and to demonstrate the interplay between offsets and guard band.

The parameters are described in Table 4. We vary the propagation time (P), the jitter of the propagation ($2p$), the upper bound of the switching time ($\overline{z}$) and the parameters of the clocks (Δ, η, ρ). All nodes have the same parameters ($\forall i, j, \underline{P}_{i,j} = P - p, \overline{P}_{i,j} = P + p, \Delta_i = \Delta, \eta_i = \eta, \rho_i = \rho$). The "perfect" values correspond to ideal clocks and negligible switching time. Except if mentioned otherwise, if a configuration is said "perfect" [resp. "default"], all parameters have the perfect [resp. default] values as in Table 4.

The time offsets are defined up to a common time shift, and we set $o_1 = 0$ in all experiments.

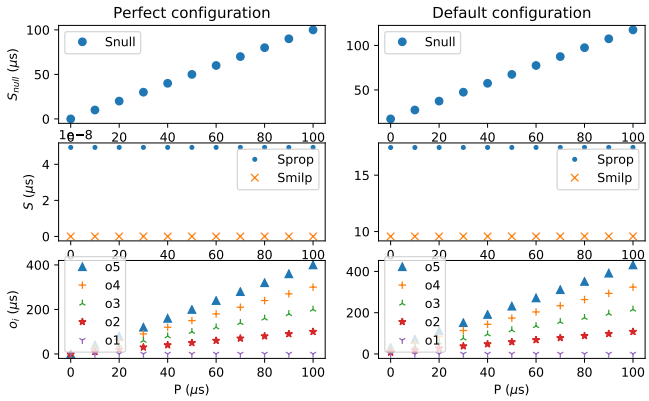

Fig. 8: Exp L.1: Guard bands (upper panels) and optimal offsets (bottom panel) versus mean propagation time P (Line topology).

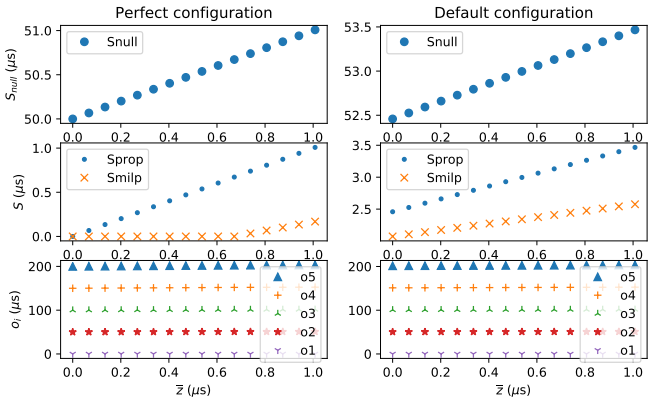

Fig. 10: Exp L.3: Guard bands (upper panels) and optimal offsets (bottom panel) versus upper bound on switching delay $\overline{z}$ (Line topology).

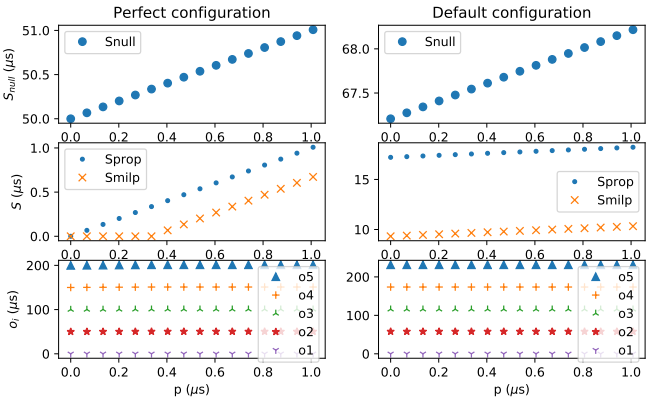

Fig. 9: Exp L.2: Guard bands (upper panels) and optimal offsets (bottom panel) versus propagation jitter parameter p (Line topology).

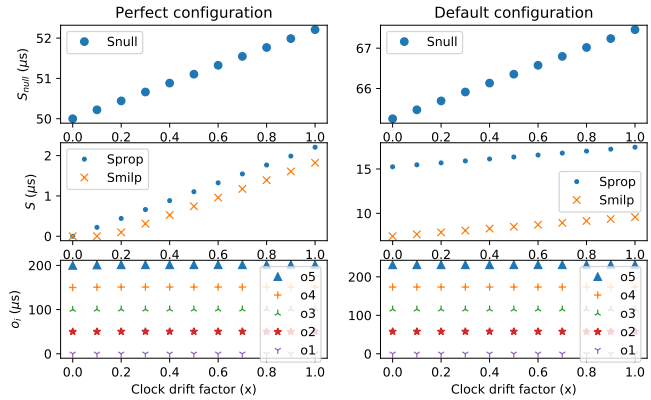

Fig. 11: Exp L.4: Guard bands (upper panels) and optimal offsets (bottom panel) versus clock nonideality factor x, where $\Delta = x\mu$s, $\eta = 2x$ns, $\rho = 1 + 10^{-4}x$ (Line topology).

6.1 Line

We start with the simple line illustrated in Figure 7a. Each experiment considers a perfect and a default configuration and varies one parameter. Figures 8 to 11 plot S_{null} (upper line), S_{prop} and S_{milp} (medium line) as well as the optimal offsets computed by the MILP (bottom line). The left row presents the perfect configuration, and the right row presents the default configuration.

- Experiment L.1, Figure 8: The propagation time P varies from 0 to 0.1ms by steps of 10μs.
  Observations: For the perfect configuration, the guard band with all null offsets S_{null} grows up linearly with the propagation time. In contrast, the guard bands computed by absorbing the propagation time or using the MILP are quasi null: the MILP computes null values, and the others return the tolerance ϵ. The MILP computes the sames offsets as the heuristics based on propagation absorption, setting $o_{i+1} = o_i + P_{i+1,i}$.
  The introduction of non null jitters and imperfect clocks does not change the trends but increases the guard band values: the MILP computes a guard band S_{milp} around 10μs whereas the propagation absorption heuristics computes S_{prop} around 18μs. The offsets computed by the MILP are also slightly increased.
- Experiment L.2, Figure 9: The propagation jitter parameter p varies from 0 to 1.5 times $\underline{E}$ by steps of 0.1.
  Observations: In the perfect configuration, S_{null} and S_{prop} increase linearly w.r.t. the semi-variation of the propagation p. When $p \leq \frac{\underline{E}}{2}$ the MILP solver finds a null guard band by setting $o_{i+1} = o_i + P_{i+1,i} + p$. But as shown by Prop. 1, if $p > \frac{\underline{E}}{2}$ which is equivalent to $2p = \overline{P} - \underline{P} > \underline{E}$, S cannot be null. Then the MILP solver finds $S = p - \frac{\underline{E}}{2}$ and $o_{i+1} = o_i + P + \frac{\underline{E}}{2}$.
  For the default configuration, we also see a linear increase, but starting at higher values, as in experiment L.1.
- Experiment L.3, Figure 10: The switching time upperbound $\overline{z}$ varies from 0 to 1.5 times $\underline{E}$ by steps of 0.1.
  Observations: In the perfect configuration, S_{null} and S_{prop} increase linearly w.r.t. the maximal switching time $\overline{z}$. In the perfect configuration, as long as $\overline{z} < \underline{E}$, the MILP solver finds a null guard, by setting $o_{i+1} = o_i + P_{i,j} + \overline{z}_j$. But as shown by Prop. 1, if $\overline{z} > \underline{E}$, S cannot be null. The choice of the offset still com-

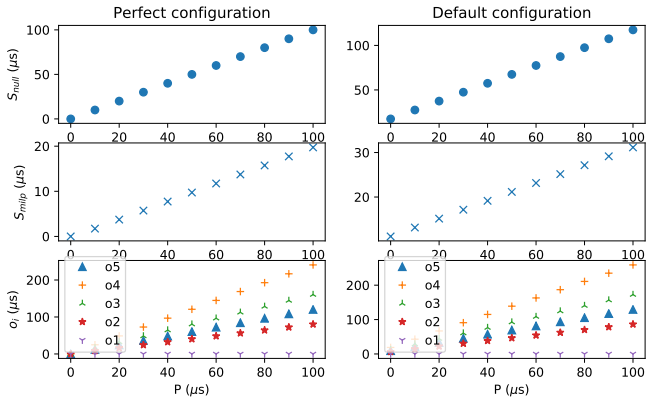

Fig. 12: Exp F.1: Guard bands (upper panels) and optimal offsets (bottom panel) versus mean propagation time P (Feed-forward topology).

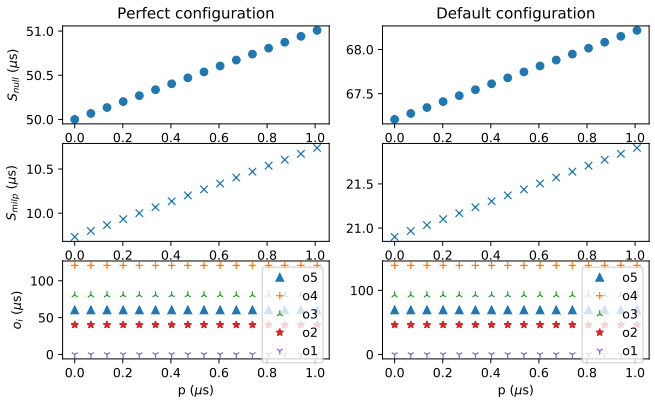

Fig. 13: Exp F.2: Guard bands (upper panels) and optimal offsets (bottom panel) versus propagation jitter parameter p (Feed-forward topology).

pensates the propagation, minus a compensation term $o_{i+1} \approx o_i + P_{i,j} + \frac{\underline{E}+\overline{z}}{2}$.
In the default configuration, we also see a linear increase, but starting at higher values, as in experiment L.1. It appears that the slopes are not the same: the MILP solver uses the offsets values to absorb a part of the jitter.

- Experiment L.4, Figure 11: The clock quality depends on a parameter x and ranges from perfect ($x = 0$) to default ($x = 1$) by steps of 0.1 ($\Delta = x\mu$s, $\eta = 2x$ns, $\rho = 1 + 10^{-4}x$).
Observations: Here, too, the guard band value increases linearly with same slope for all cases. The MILP solver sets $o_{i+1} - o_i = P$ and uses the guard band value to absorb the clock imprecision. Clock nonideality adds several microseconds to the guard band but has little effect on the optimal offsets.

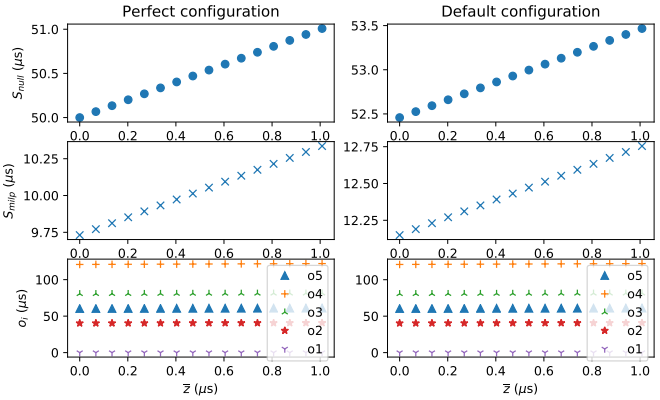

Fig. 14: Exp F.3: Guard bands (upper panels) and optimal offsets (bottom panel) versus upper bound on switching delay $\overline{z}$ (Feed-forward topology).

6.2 Feed-forward with two paths

We consider next the topology on Figure 7b, which has parallel paths. It follows that the propagation absorption heuristics cannot be applied: it is no longer possible to set the downstream offset as the sum of the upstream offset and the propagation time since SW4 has two upstream offsets. Therefore, in Figures 12 to 15 we compare only the values of S_{null} and S_{milp}. We vary the same factors as with the line topology.

- Experiment F.1, Figure 12: The propagation time P varies from 0 to 0.1ms by steps of 10μs.
Observations: In the perfect configuration, as with the line configuration, S_{null} increases as a linear function of P, from 0 to 100μs. The optimal solution has $o_{i+1} = o_i + P$ on the shortest path and distributes the offsets along the longest path. The guard band S_{milp} increases to absorb the difference, from 0 to 20μs, and is 5 times less than with the null heuristic.
The default configuration has similar trends, but must compensate the clock imperfections.
- Experiment F.2, Figure 13: The propagation jitter parameter p varies from 0 to 1.5 times $\underline{E}$ by steps of 0.1.

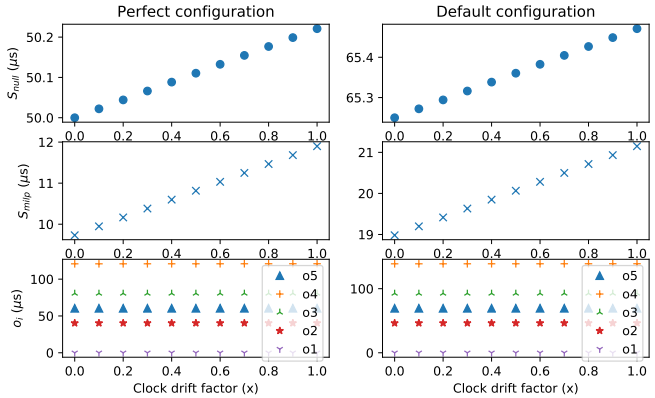

Fig. 15: Exp F.4: Guard bands (upper panels) and optimal offsets (bottom panel) versus clock nonideality factor x, where $\Delta = x\mu$s, $\eta = 2x$ns, $\rho = 1 + 10^{-4}x$ (Feed-forward topology).

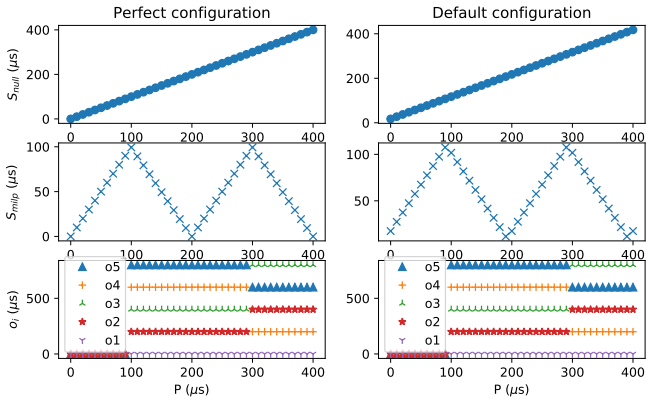

Fig. 16: Exp R.1: Guard bands (upper panels) and optimal offsets (bottom panel) versus mean propagation time P (Ring topology).

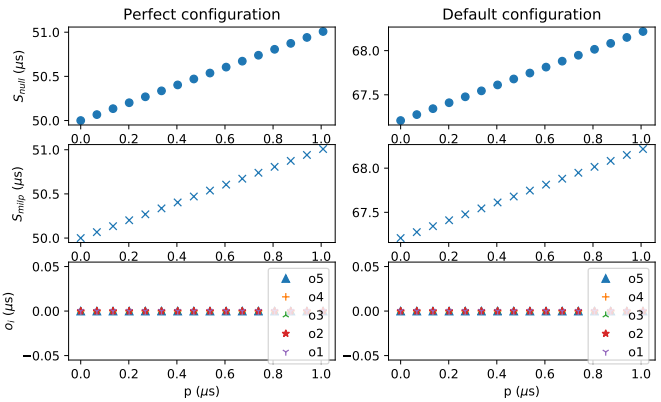

Fig. 17: Exp R.2: Guard bands (upper panels) and optimal offsets (bottom panel) versus propagation jitter parameter p (Ring topology).

Observations: As with previous cases, S_{null} increases as a linear function of p. This is also the case for S_{milp}: the optimal solution uses the same strategy as in F.1, namely, the optimal offsets compensate the propagation difference between the two paths, and S is increased to absorb the propagation jitter.

- Experiment F.3, Figure 14: The switching time upper-bound $\overline{z}$ varies from 0 to 1.5 times $\underline{E}$ by steps of 0.1.
  Observations: The results are very similar, except that the S_{milp} values are smaller (from 22.25μs to 23μs).
- Experiment F.4, Figure 15: The clock quality depends on a parameter x and ranges from perfect ($x = 0$) to default ($x = 1$) by steps of 0.1 ($\Delta = x\mu$s, $\eta = 2x$ns, $\rho = 1 + 10^{-4}x$).
  Observations : The results are very similar to previous experiments. In particular, clock nonideality adds several microseconds to the guard band but has little effect on the optimal offsets.

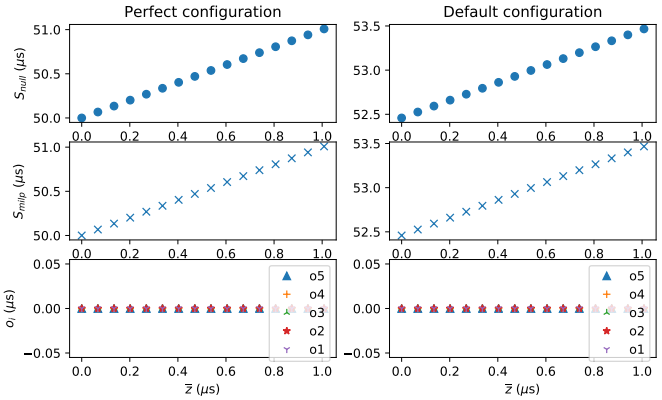

Fig. 18: Exp R.3: Guard bands (upper panels) and optimal offsets (bottom panel) versus upper bound on switching delay $\overline{z}$ (Ring topology).).

6.3 Ring

Last, we consider the ring topology in Figure 7c, which is the simplest topology with cyclic dependencies. Here, too, the propagation absorption heuristics cannot be applied as it requires to set the downstream offset to the sum of the upstream offsets, leading to a circular condition that has no solution. Therefore, in Figures 16 to 19 we compare only the values of S_{null} and S_{milp}. We vary the same factors as with the line topology.

- Experiment R.1, Figure 16: The propagation time P varies from 0 to 0.4ms by steps of 10μs. The range, here, is increased to see the specific behaviour of S_{MILP}.
  Observations: As with the previous experiments, the strategy based on null offsets creates a S_{null} that increases linearly to compensate the propagation time. When the propagation time is equal to 40% of the cycle time, 80% of the bandwidth is lost.
  In contrast, the optimal value found by the MILP uses a different strategy. In the perfect configuration, when $P \in [0; 100\mu\text{s}]$, i.e. when $5P \in [0; T/2]$, the null offset is optimal and $S_{\text{null}} = S_{\text{milp}}$. This goes until $5P = T/2$,

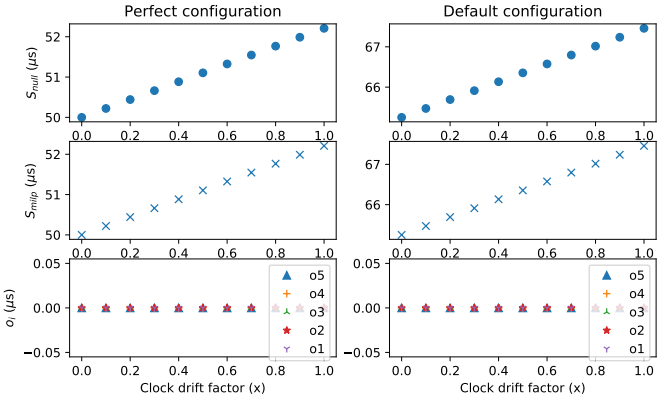

Fig. 19: Exp R.4: Guard bands (upper panels) and optimal offsets (bottom panel) versus clock nonideality factor x, where $\Delta = x\mu$s, $\eta = 2x$ns, $\rho = 1 + 10^{-4}x$ (Ring topology).

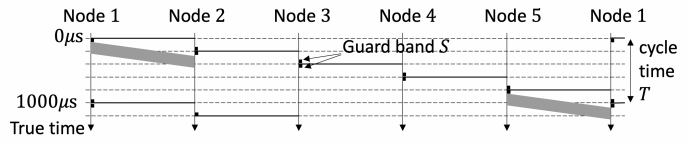

Fig. 20: Ring topology: illustration of optimal offsets and guard band when the mean propagation time is $P = 150\mu$s, with otherwise default configuration. A frame sent by node 1 is received in the same cycle whereas a frame sent by node 5 is received in the next cycle.

where 20% of the bandwidth is lost due to the guard band at the beginning and the end of each cycle. However, beyond this point, i.e. when $5P \in (T/2; T]$, the optimal solution sets $o_{i+1} = o_i + T/5$, i.e. the cycle time is uniformly distributed among the offsets and the guard band value decreases, down to the optimal case, when the total propagation time $5P$ is equal to the cycle time T. Then when P increases beyond this value, the minimal guard band increases again and the process repeats. The loss of bandwidth oscillates between 0 and 20%, whereas with the null offset heuristic, it increases linearly well beyond 20% (up to a point where the null heuristic has no feasible guard band whereas the MILP solver always finds a solution.)
With the (realistic) default configuration, we see the same pattern but with some additional margin to account for the other non null parameters. It is enlightening to analyze the spatial distribution of offsets, as shown in Figure 20. Here the offsets are used to absorb the cycle time, and there is an index jump from node 5 to node 1, namely, a frame sent in cycle k_5 at node 5 is received in cycle $k_1 = k_5 + 1$ at node 1. A cycle jump does not occur when $P \leq 100\mu$s but always occurs beyond.

- Experiment R.2, Figure 17: The propagation jitter parameter p varies from 0 to 1.5 times $\underline{E}$ by steps of 0.1. *Observations:* Like in previous experiments, S_{null} increases linearly to compensate the propagation jitter. The optimal solution also selects null offsets, because the sum of the propagation time is smaller than half of the period ($5P \ll \frac{T}{2}$) and consequently S_{milp} also compensates the propagation jitter.
- Experiment R.3, Figure 18: The switching time upperbound $\overline{z}$ varies from 0 to 1.5 times $\underline{E}$ by steps of 0.1. and $P = 50\mu s$.
Observations: The results are very similar to the experiment R.2, but the guard bands are smaller in the default configuration.
- Experiment R.4, Figure 19: The clock quality depends on a parameter x and ranges from perfect ($x = 0$) to default ($x = 1$) by steps of 0.1 ($\Delta = x\mu$s, $\eta = 2x$ns, $\rho = 1 + 10^{-4}x$).
Observations: The results are very similar to experiments R.2 and R.3. We also see that clock nonidealities add up to 15 microseconds to the guard band.

6.4 Summary of Observations

A few lessons can be learnt from these experiments.

1) The choice of the offsets can dramatically reduce the guard band.
2) The nonideality parameters of clock, switching delay and propagation jitter affect the guard band; ignoring them leads to too small guard band.
3) In contrast, the values of the offsets are mainly influenced by topology and propagation latency, not significantly by other parameters.

Some other trends can be derived directly from the equations, without running experiments. In the experiments, all nodes and all links have the same characteristics. This should not be the case in reality. Since the guard band value S should respect the condition for every pair source/receiver, the one with the larger value will impose it to all nodes (e.g. if a single node is badly synchronised, all nodes in the network must take it into account in their own guard band).

The propagation time deserves a specific discussion. If the propagation times are different (because of different cable length for example), the null offset heuristic will lead to take into account the maximal propagation time in all nodes, whereas the heuristic absorbing propagation with offset can compensate the propagation time per link (but this heuristic can not be used for any topology). The MILP will also try to allocate offsets on each node in order to compensate the propagation delay of each link.

6.5 Computing the Guard Band in Practice

We have presented 3 methods to compute the guard band:

- either setting null offsets in all nodes, and use the guard band value S_{null}, defined in eq. (45),
- or setting offsets in order to absorb the propagation time, and use the guard band value S_{prop}, defined in eq. (54),
- or use a MILP solver, presented in Problem (P-MILP).

The use of null offsets is the simplest, and can be used as long as the propagation time is small w.r.t. the cycle time (cf. (39)), but it will not give the best value since the guard band must absorb this propagation time (cf. Exp L.1, Exp F.1 and Exp R.1 presented respectively in Fig. 8, 12 and 16).

Setting offsets in order to absorb the propagation time allows to compensate this effect, but this is not possible for any topology (it is not possible if there exist two paths with different cumulated propagation times or if there are cyclic dependencies).

The last solution consist in using the MILP. One common drawback of MILP is the computation time. But thanks to its simplicity, the one presented in Problem (P-MILP) can be solved in a very short time. Each configuration presented in the experiment section is solved in less than 10ms (using `lp_solve` on a i5 /2.70GHz CPU, the `time` command returns 0.00). To challenge the computation time, we have enlarged the ring topology to consider rings from 5 to 50 nodes with step 5. Each MILP was solved in less than 80ms.

The three methods have been evaluated on simple topologies to show the applicability of the approach and they have permitted to illustrate some trends. Now that these tools have been provided, it would be of interest,

in future studies, to evaluate the performance of CQF on real topologies. In these simple cases, the guard band may represent 20% of the bandwidth ($2 \cdot 100\mu s$ over 1ms), but it is unclear if it can occur in real configurations. It also gives an opportunity to compare CQF and other proposals, presented in Section 7.

Last, there exists a minimal granularity associated with the GCL: `TickGranularity` [9, §8.6.9.4.16] and the method may compute a guard band S that is not a multiple of `TickGranularity`. But thanks to Thm. 2, if S is a solution of Thm. 1, then $S_T = \texttt{TickGranularity} \left\lceil \frac{S}{\texttt{TickGranularity}} \right\rceil$ also is, as long as $S_T \leq \overline{S}$.

7 Related work

Several extensions of CQF have been proposed, like CQF 3-queues [18], Paternoster [19], Large-Scale Deterministic Network (LDN, [20], [21]), Cycle Specified Queuing and Forwarding (CSQF, [22]) and Tagged Cyclic Queuing and Forwarding (TCQF, [23]). A global survey, up to 2019, can be found in [2].

All these extensions have been designed to overcome some limitations of CQF, but it seems that all authors consider that all CQF nodes have to align their cycle time, i.e. have to share the same offset (cf. Section 5.1.1), whereas the standard does not explicitly state so.

Also note that all these extensions (except TCQF) use 3 or even 4 queues, whereas Ethernet/TSN offers only 8 queues (or even less, depending on the implementation). Since a real-time network may have many types of traffic, each with specific requirements, the mapping from traffic types to only 8 TSN classes may become an issue [24]. TCQF relies on MPLS tagging.

While CQF offers bounded jitters ($2T$), some flows requires very small jitters. For such flow, TSN allows to configure the GCLs to provide a Time-Triggered forwarding, commonly called Time Aware Shaping (TAS) [25], [26]. The Time-Aware Cyclic-Queuing (TACQ) proposes to integrate both a TAS-like mechanism and CQF on an output port by closing both CQF queues at start of cycle to allow low jitter flows to be forwarded [27]. To optimise the bandwidth usage, it would be natural to overlap this closing time and the guard band.

A comparison between CQF and CBS on an automotive use case is done by simulation in [28], but without any consideration on the guard band.

The computed bounds assume that each CQF buffer does not receive in one cycle more than what can be sent in the next cycle. The Injection Time Planning (ITP) mechanism computes the global cycle time and per-flow offsets for periodic flows in order to maximise the admissible load while satisfying this constraint [29]. The approach is generalised in [30] by adding in each End-System an "adapter" in charge of implementing the injection using a list of queues, and also by providing an online algorithm. It assumes that all offsets are equal, and the guard band only has to absorb the clock synchronization precision.

8 Conclusion

The expected behaviour of CQF requires some time alignments between cycles, using appropriate values of the guard band and the nodal offsets. We provided a mathematically proven method to effectively compute such values, while accounting for clock nonidealities and jitters. Illustrative case studies indicate that clock nonidealities have a non-negligible influence and should not be ignored.

9 Proofs

All the proofs are in the supplementary material. They can also be found in the appendix of [31].

References

[1] "IEEE Standard for Local and metropolitan area networks–Bridges and Bridged Networks–Amendment 29: Cyclic Queuing and Forwarding," IEEE, IEEE Standard 802.1Qch, 2017.

[2] A. Nasrallah, V. Balasubramanian, A. S. Thyagaturu, M. Reisslein, and H. ElBakoury, "Cyclic queuing and forwarding for large scale deterministic networks: A survey," *ArXiv, vol. abs/1905.08478*, 2019.

[3] B. Jonsson, S. Perathoner, L. Thiele, and W. Yi, "Cyclic dependencies in modular performance analysis," in *Proc. of the 8th Int. Conf on Embedded Software (EMSOFT'08)*. ACM Press, 2008, pp. 179–188. [Online]. Available: http://doi.acm.org/10.1145/1450058.1450083

[4] D. Starobinski, M. Karpovsky, , and L. Zakrevski, "Application of Network Calculus to General Topologies using Turn-Prohibition," in *Proceeding of the 21st Annual Joint Conference of the IEEE Computer and Communications Societies*, June 2002, pp. 411–421.

[5] L. Thomas, J.-Y. Le Boudec, and A. Mifdaoui, "On Cyclic Dependencies and Regulators in Time-Sensitive Networks," in *IEEE Real-Time Systems Symposium, RTSS 2019, Hong Kong, SAR, China, December 3-6, 2019*. IEEE, 2019, pp. 299–311. [Online]. Available: https://doi.org/10.1109/RTSS46320.2019.00035

[6] L. Thomas and J.-Y. Le Boudec, "On time synchronization issues in time-sensitive networks with regulators and nonideal clocks," *Proceedings of the ACM on Measurement and Analysis of Computing Systems*, vol. 4, no. 2, pp. 1–41, 2020.

[7] A. Nasrallah, V. Balasubramanian, A. S. Thyagaturu, M. Reisslein, and H. ElBakoury, "Cyclic queuing and forwarding for large scale deterministic networks: A survey," *ArXiv, vol. abs/1905.08478*, 2019.

[8] "IEEE standard for local and metropolitan area networks–bridges and bridged networks–amendment 28: Per-stream filtering and policing," IEEE, Standard 802.1Qci, 2017.

[9] "IEEE standard for local and metropolitan area networks–bridges and bridged networks–amendment 25: Enhancements for scheduled traffic," IEEE, IEEE Standard 802.1Qbv, 2015.

[10] "IEEE standard for local and metropolitan area networks – bridges and bridged networks – amendment 26: Frame preemption," IEEE Standard 802.1Qbu, 2016.

[11] D. Thiele and R. Ernst, "Formal worst-case performance analysis of time-sensitive ethernet with frame preemption," in *2016 IEEE 21st International Conference on Emerging Technologies and Factory Automation (ETFA)*. IEEE, 2016, pp. 1–9.

[12] N. Finn, "Mutiple Cyclic Queuing and Forwarding," IEEE 802.1 Working Group, Tech. Rep. df-finn-multiple-CQF-0919-v01, September 2019. [Online]. Available: https://www.ieee802.org/1/files/public/docs2019/df-finn-multiple-CQF-0919-v01.pdf

[13] "IEEE/ISO/IEC International Standard for Information technology–Telecommunications and information exchange between systems–Local and metropolitan area networks–Part 1AS:Timing and synchronization for time-sensitive applications in bridged local area networks, ISO/IEC/IEEE 8802-1AS:2021(E)," 2021.

[14] NXP, *SJA1105 5-port automotive Ethernet switch*, November 2016. [Online]. Available: https://www.nxp.com/docs/en/data-sheet/SJA1105.pdf

[15] N. D. (ND), *Intel®Ethernet Controller I210 Datasheet*, January 2021. [Online]. Available: https://www.intel.com/content/www/us/en/content-details/333016/intel-ethernet-controller-i210-datasheet.html

[16] AEEC, "ARINC 664 P7-1: Aircraft data network, part 7, avionics full-duplex switched ethernet network," Airlines Electronic Engineering Committee, Tech. Rep., september 2009.

[17] "IEEE standard for local and metropolitan area networks – bridges and bridged networks," IEEE, IEEE Standard 802.1Q, 2018.

[18] N. Finn, E. Mohammadpour, J. Zhang, and B. Varga, "RFC 9320 Deterministic Networking (Detnet) Bounded Latency," 2022.

[19] M. Seaman, "Paternoster policing and scheduling," IEEE, Tech. Rep., May 2019, revision 2.1. [Online]. Available: https://grouper.ieee.org/groups/802/1/files/public/docs2019/cr-seaman-paternoster-policing-scheduling-0519-v04.pdf

[20] L. Qiang, X. Geng, B. Liu, T. Eckert, L. Geng, and G. Li, "Large-Scale Deterministic IP Network," IETF, Internet-Draft draft-qiang-detnet-large-scale-detnet-05, 2019. [Online]. Available: https://datatracker.ietf.org/doc/html/draft-qiang-detnet-large-scale-detnet-05

[21] B. Liu, S. Ren, C. Wang, V. Angilella, P. Medagliani, S. Martin, and J. Leguay, "Towards large-scale deterministic ip networks," in *2021 IFIP Networking Conference (IFIP Networking)*, 2021, pp. 1–9.

[22] M. G. Chen, Gengn Xuesong, and Z. Li, "Segment Routing (SR) Based Bounded Latency," IETF, Internet-Draft draft-chen-detnet-sr-based-bounded-latency-01, May 2019. [Online]. Available: https://datatracker.ietf.org/doc/html/draft-chen-detnet-sr-based-bounded-latency-01

[23] T. Eckert, S. Bryant, A. G. Malis, and G. Li, "Deterministic Networking (DetNet) Data Plane - Tagged Cyclic Queuing and Forwarding (TCQF) for bounded latency with low jitter in large scale DetNets," Internet Engineering Task Force, Internet-Draft draft-eckert-detnet-tcqf-01, Nov. 2022, work in Progress. [Online]. Available: https://datatracker.ietf.org/doc/draft-eckert-detnet-tcqf/01/

[24] "Time-Sensitive Networking Profile for Industrial Automation," IEEE 802, Tech. Rep., 2021.

[25] S. S. Craciunas, R. S. Oliver, M. Chmelík, and W. Steiner, "Scheduling real-time communication in IEEE 802.1Qbv time sensitive networks," in *Proceedings of the 24th International Conference on Real-Time Networks and Systems (RTNS'16)*, ser. RTNS'16. New York, NY, USA: Association for Computing Machinery, 2016, pp. 183–192. [Online]. Available: https://doi.org/10.1145/2997465.2997470

[26] P.-J. Chaine and M. Boyer, "Shortening gate closing time to limit bandwidth waste when implementing Time-Triggered scheduling in TAS/TSN," in *Proc. of the 15th Junior Researcher Workshop on Real-Time Computing*, Paris, France, 2022. [Online]. Available: https://rtns2022.inria.fr/files/2022/06/proceedings_jrwrtc2022_final.pdf

[27] Y. Huang, S. Wang, B. Wu, T. Huang, and Y. Liu, "TACQ: Enabling Zero-jitter for Cyclic-Queuing and Forwarding in Time-Sensitive Networks," in *ICC 2021 - IEEE International Conference on Communications*, 2021, pp. 1–6.

[28] L. Leonardi, L. L. Bello, and G. Patti, "Performance assessment of the IEEE 802.1Qch in an automotive scenario," in *Proc. of the AEIT Int. Conf. of Electrical and Electronic Technologies for Automotive (AEIT AUTOMOTIVE)*, 2020, pp. 1–6.

[29] J. Yan, W. Quan, X. Jiang, and Z. Sun, "Injection time planning: Making CQF practical in time-sensitive networking," in *Proc. of the 39th IEEE Conference on Computer Communications (INFOCOM 2020)*, 2020, pp. 616–625.

[30] W. Quan, J. Yan, X. Jiang, and Z. Sun, "On-line traffic scheduling optimization in IEEE 802.1 Qch based time-sensitive networks," in *Proc. of the Int. Conf. on High Performance Computing and Communications; Int. Conf. on Smart City; 6th Int. Conf. on Data Science and Systems (HPCC/SmartCity/DSS)*. IEEE, 2020, pp. 369–376.

[31] D. Guidolin-Pina, M. Boyer, and J.-Y. Le Boudec, "Configuration of Guard Band and Offsets in Cyclic Queuing and Forwarding," Sep. 2022, working paper or preprint. [Online]. Available: https://hal.science/hal-03772877

[32] J. Liebeherr *et al.*, "Duality of the max-plus and min-plus network calculus," *Foundations and Trends® in Networking*, vol. 11, no. 3-4, pp. 139–282, 2017.

Damien GUIDOLIN--PINA is an industrial PhD student at RealTime-at-Work since 2021, with academic enrollment at ISAE SUPAERO. His academic supervisor is Marc Boyer (Onera/DTIS). He received an engineering degree from ISAE ENSMA, Poitiers, France, in 2020. He then joined RealTime-at-Work, a French software editor helping OEMs and Tier1s design safe & cost optimized Electrical/Electronic (E/E) communication architectures for 10 months as a software engineer working on implementing some IEEE TSN features in RTaW-PEGASE, an industry-leading platform for the design, configuration, and simulation of embedded communication architectures. His research focuses on the performance of real-time communication systems, mainly using the Network Calculus theory.

Marc BOYER received the Engineering degree in computer science from Toulouse INP-ENSEEIHT, Toulouse, France, in 1996, and the Ph.D. degree in computer science from the Université Paul Sabatier Toulouse III, Toulouse, in 2001. He was an Assistant Professor with the Network Department, Toulouse INP-ENSEEIHT, from 2002 to 2008. He is currently a Research Scientist with the Office National d'Etudes et de Recherches Aérospatiales (ONERA), Toulouse. His research interests focuses on embedded networks (AFDX, TSN) and the performances of these networks, mainly using the network calculus theory.

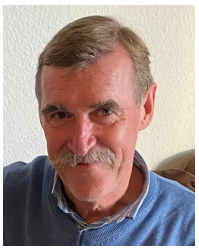

Jean-Yves LE BOUDEC is professor at EPFL and fellow of the IEEE. He graduated from Ecole Normale Supérieure de Saint-Cloud, Paris, where he obtained the Agrégation in Mathematics with rank 4 in 1980, and received his doctorate in 1984 from the University of Rennes, France. From 1984 to 1987 he was with INSA/IRISA, Rennes. In 1987 he joined Bell Northern Research, Ottawa, Canada, as a member of scientific staff in the Network and Product Traffic Design Department. In 1988, he joined the IBM Zurich Research Laboratory where he was manager of the Customer Premises Network Department. In 1994 he became associate professor at EPFL. His interests are in the performance and architecture of communication systems and smart grids. He co-authored a book on network calculus, which serves as a foundation for deterministic networking, an introductory textbook on Information Sciences, and is the author of the book "Performance Evaluation". He received numerous awards, among which the IEEE millenium medal, the Infocom Best Paper award, the ACM Sigmetrics Best Paper award, the ACM Conext Best Paper Award, the IEEE Communication Society William R. Bennett Prize, the IEEE Security and Privacy Test-of-Time award and the EPFL I&C Best Teacher Award.